Quantum Science and Technology

PAPER

Time molecules with periodically driven interacting qubits

To cite this article: K V Shulga *et al* 2021 *Quantum Sci. Technol.* **6** 035012

View the article online for updates and enhancements.

IOP ebooks™

Bringing together innovative digital publishing with leading authors from the global scientific community.

Start exploring the collection–download the first chapter of every title for free.

This content was downloaded from IP address 134.75.87.181 on 12/08/2021 at 03:35

Quantum Science and Technology

PAPER

Time molecules with periodically driven interacting qubits

RECEIVED
4 December 2020

REVISED
2 May 2021

ACCEPTED FOR PUBLICATION
10 May 2021

PUBLISHED
17 June 2021

K V Shulga[1,*], I Vakulchyk[2,3], Y Nakamura[1,4], S Flach[2,3] and M V Fistul[2,5,6]

[1] Center for Emergent Matter Science (CEMS), RIKEN, Wako-shi, Saitama 351-0198, Japan
[2] Center for Theoretical Physics of Complex Systems, Institute for Basic Science (IBS), Daejeon 34126, Republic of Korea
[3] Basic Science Program, Korea University of Science and Technology (UST), Daejeon 34113, Republic of Korea
[4] Research Center for Advanced Science and Technology (RCAST), The University of Tokyo, Tokyo 153-8904, Japan
[5] Theoretische Physik III, Ruhr-Universität Bochum, Bochum 44801, Germany
[6] National University of Science and Technology 'MISIS', Russian Quantum Center, Moscow 119049, Russia
[*] Author to whom any correspondence should be addressed.

E-mail: kirill_shulga@protonmail.ch

Keywords: quantum interference effects, quantum entanglement, superconducting qubits

Abstract

We provide numerical evidence for a temporal quantum-mechanical interference phenomenon: time molecules (TMs). A variety of such stroboscopic states are observed in the dynamics of two interacting qubits subject to a periodic sequence of π-pulses with the period T. The TMs appear periodically in time and have a large duration, $\delta t_{\rm TM} \gg T$. All TMs are characterized by almost zero value of the total polarization and a strong enhancement of the entanglement entropy S up to the maximum value of $S \simeq \ln 2$ indicating the presence of corresponding Bell state. Moreover, the TMs demonstrate a stroboscopic switching between the two maximally entangled Bell states and a slow leakage into other eigenstates. The TMs are generated by the commensurability of the Floquet eigenvalues and the presence of maximally entangled Floquet eigenstates. The TMs remain stable with detuned system parameters and with an increased number of qubits. In particular, we observed the TMs in the dynamics of three interacting qubits, and these TMs show a stroboscopic switching between the four Greenberger–Horne–Zeilinger states. The TMs can be observed in microwave experiments with an array of superconducting qubits.

1. Introduction

Great attention has been devoted to an experimental and theoretical study of coherent quantum dynamics of the various quantum system subject to a time-periodic external perturbation, i.e., so-called *Floquet quantum systems* [1–3]. A large amount of spectacular quantum phenomena, e.g., the microwave-induced Rabi oscillations [4], the ac Stark effect, the dynamic quantum tunneling [1, 2], and the quantum ratchet effect [3], to name a few, has been predicted, analyzed and observed in different condensed matter and optical systems.

Most of these effects that can be called temporal quantum interference and demonstrate long-living oscillations of the physical quantities. The frequency of such oscillations is substantially different from the one of the applied time-periodic external potential. For example, microwave-induced Rabi oscillations for the single particle have been observed for nuclear spins driven by a resonant ac magnetic field [4]. The frequency of these Rabi oscillations is much smaller than the frequency of the applied microwave radiation. Also, more complex temporal quantum interference patterns such as Ramsey fringes [5] and spin echo [6] occur in quantum systems driven by a periodic sequence of dc or ac pulses. Note that these interference patterns have also been observed in various macroscopic artificially prepared two-level qubit systems [7–9]. The Floquet eigenvalues of the system determine the frequency of these oscillations [1, 2].

An even wider variety of temporal interference patterns can be expected to occur in periodically driven quantum systems composed of many interacting quantum particles [10–14]. Thus, different non-equilibrium coherent quantum phases and quantum phase transitions between them were predicted in various spatially extended Floquet quantum systems [10, 11, 15, 16]. These quantum phases display a broken temporal-translation symmetry of the underlying time-periodic perturbation and an enhanced

© 2021 IOP Publishing Ltd

quantum entanglement. Here, the analogy can be drawn with with the quantum entanglement of spatially extended equilibrium quantum systems, which is strongly enhanced as the system is tuned towards a quantum phase transition point [17, 18]. The Floquet quantum systems [2] have attracted even more attention recently due to the prediction [19–21] of a novel coherent quantum state—the time crystal [22–26]. Subsequent observations [27, 28] were reported in atomic and solid-state systems. Such time crystals show stable quantum sub-harmonic oscillations with period nT (here, n is a natural number), where T is the period of an applied pulse-sequence, in spite of the unavoidable disorder and pulse-sequence imperfection. In reference [23] the firm relationship between this effect and equally spaced Floquet quasienergies with the minimum energy difference is equal to $2\pi/(nT)$, has been established.

Therefore, next questions that naturally arise in this field: is it possible to obtain complex temporal interference pattern for a few interacting particles? What is the relationship between these temporal interference patterns and the specific properties of Floquet quasienergies and eigenstates?

To answer these questions in this paper, we present numerical simulations of the coherent quantum dynamics of periodically driven qubit chains consisting of a few interacting qubits. The drive is provided by an externally applied periodic sequence of short spin-flip pulses. We observe various temporal interference patterns in the total polarization of the qubits measured at stroboscopic times. These interference patterns depend strongly on two important parameters of the problem—the interaction strength between the qubits and the spin-flip pulse imperfection. For a suitable set of these parameters, we obtain dynamical states coined *time molecules* (TMs). TMs appear periodically in time, have a long duration, $\delta t_{\mathrm{TM}} \gg T$, and show an almost zero value of the total polarization and a quantum entanglement entropy close to the maximal value, $S \simeq \ln 2$. The latter observation indicates that the TMs are in one of the maximally entangled states. For example for two interacting qubits the observed TMs are in one of the Bell states and demonstrate stroboscopic switching between two Bell states. Similarly, for a system composed of three interacting qubits, we obtain stroboscopic switching between four different Greenberger–Horne–Zeilinger (GHZ) states [29, 30]. The analysis of the Floquet eigenvalues and eigenstates allows us to explain the formation and the dynamical properties of TMs. Such TMs can be directly observed in two-tone dispersive measurements of short arrays of interacting superconducting qubits.

2. Model and numerical procedure

Let us consider a one-dimensional chain of N interacting qubits, i.e., artificially fabricated two-level systems subject to a periodic sequence of spin-flip pulses. The period of the pulse sequence is T. The time-dependent Hamiltonian acting over a single period T is written in the spin representation as

$$\begin{aligned}
&\hat{H}_{\mathrm{sys}} = \hat{H}_1 + \hat{H}_2,\\
&\hat{H}_1 = \frac{\hbar\alpha}{2t_1}\sum_{i=1}^{N}\hat{\sigma}_{x,i}, \quad 0 < t < t_1,\\
&\hat{H}_2 = \frac{\hbar}{T-t_1}\sum_{i=1}^{N}\delta_i(\hat{\sigma}_{z,i}+1) + \frac{\hbar g}{T-t_1}\sum_{\langle i,j\rangle}(\hat{\sigma}_{x,i}\hat{\sigma}_{x,j}+\hat{\sigma}_{y,i}\hat{\sigma}_{y,j}), \quad t_1 < t < T,
\end{aligned} \tag{1}$$

where $\hat{\sigma}_{x,i}$, $\hat{\sigma}_{y,i}$ and $\hat{\sigma}_{z,i}$ are the corresponding Pauli matrices of the ith qubit and g is the dimensionless coupling strength of the exchange interaction between a pair of qubits, $\langle i,j\rangle$. A single spin-flip pulse is characterized by two parameters, the dimensionless pulse strength α and the pulse duration time t_1 ($t_1 \ll T$). The parameter α is chosen to be close to the π-pulse: $\alpha = \pi - 2\epsilon$. The parameter ϵ quantifies the imperfection of the π-pulse. The implementation of different coefficients δ_i in $\hat{H}_2$ allows one to simulate a spread of the qubit frequencies. Such model is based on the instantaneous gate approximation as the detuning and interaction between qubits are absent in the time interval, $0 < t < t_1$. The validity of such approximation is discussed in the appendix A.

The coherent Floquet dynamics of such a system is determined by the discrete time unitary map:

$$\Psi(nT) = \left[\mathrm{e}^{-\mathrm{i}\hat{H}_2(T-t_1)/\hbar}\cdot\hat{U}_\epsilon\right]^n\Psi(0), \tag{2}$$

where the unitary operator $\hat{U}_\epsilon$ is written explicitly as

$$\hat{U}_\epsilon = \bigotimes_i^N \begin{pmatrix} \sin\epsilon & -\mathrm{i}\cos\epsilon \\ -\mathrm{i}\cos\epsilon & \sin\epsilon \end{pmatrix}. \tag{3}$$

Here, $\Psi(0)$ is the wave function of an initial state, and n is the discrete time measured in units of T.

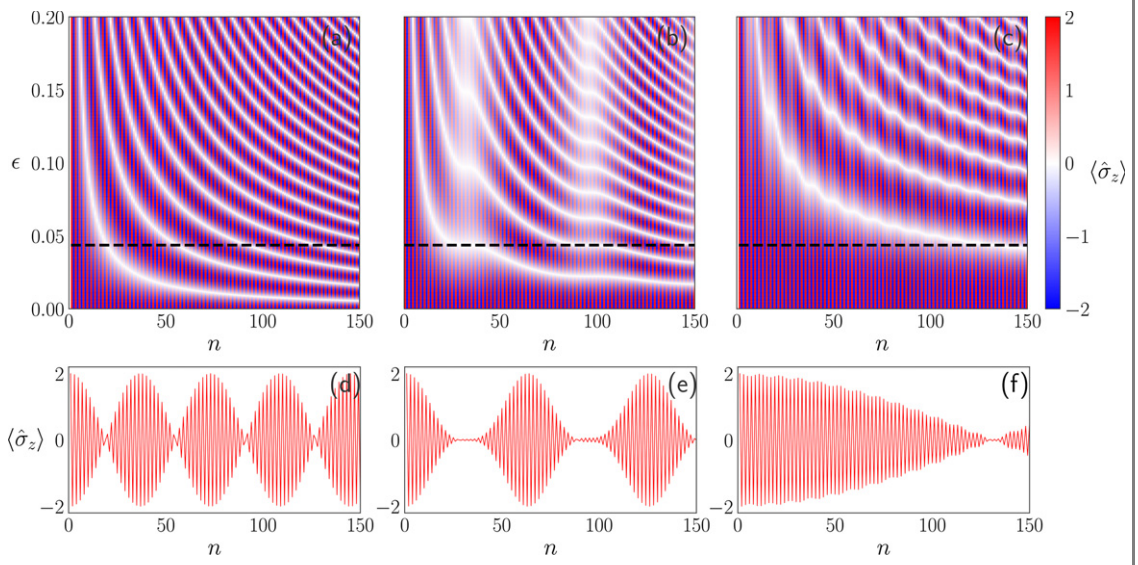

Figure 1. (a)–(c) Instantaneous total polarization $\langle\hat{\sigma}_z\rangle$ as a function of the discrete time n and the pulse imperfection ϵ for two interacting qubits. The interaction strengths are (a) $g = 0$, (b) $g = 0.05$, and (c) $g = 0.3$, respectively. The detuning $\delta_{1,2}$ between the qubits is set to zero. (d)–(f) Cross-sections of the plots in (a)–(c) at $\epsilon = 0.0436$ indicated with dashed lines.

We present numerical simulations of the above unitary map for various arrays composed of a few qubits ($N = 2, 3, 5$). The exchange interaction is provided between all pairs of qubits. We vary the parameters ϵ and g, and measure two observables: the total polarization (z-projection of the total spin) $\langle\hat{\sigma}_z\rangle = \sum_i^N \langle\hat{\sigma}_{z,i}\rangle = \langle\Psi(nT)|\sum_i^N \hat{\sigma}_{z,i}|\Psi(nT)\rangle$, and the entanglement entropy $S(nT)$ calculated by applying standard methods of quantum statistical physics (see, appendix B and [31]).

In the numerical simulations, the initial ferromagnetic state is chosen as $|\uparrow\uparrow\ldots\uparrow\rangle$. A small number of qubits and the periodic time-dependence of the Hamiltonian $\hat{H}_{\rm sys}$ (equation (1)) allows to study the dynamics of the system up to large stroboscopic times, e.g., $n > 1000$. The typical dynamics for times $0 < n < 150$ is shown in figures 1–5. The pulse-imperfection parameter ϵ is varied from 0 to 0.2.

3. Results

3.1. Total polarization

We first focus on the dynamics of *two* identical interacting qubits with $\delta_{1,2} \equiv \delta_1 - \delta_2 = 0$. For all values of interaction strength g, the dynamics shows stroboscopic oscillations with the frequency, π/T. For $g = 0$, the total polarization displays quantum beats with a large characteristic period $\pi T/(2\epsilon) \gg T$ (see the detailed analysis of quasienergies in appendix C). The quantum beats are shown in the plots of figures 1(a) and (d). Notice that at discrete times $n \approx \pi(2m+1)/(4\epsilon)$, $m = 0, 1, 2, \ldots$, the total polarization is zero (white lines in figure 1(a)). A slight increase of the interaction strength $g \ll \epsilon$ results in a distortion of the quantum oscillations, and a moderate increase of the beating period (not shown). In the opposite case $g \gg \epsilon$ the quantum beats in figures 1(c) and (f) gain very large periods $\pi g T/(2\epsilon^2)$ (see the analysis in appendix C).

A most interesting and intriguing dynamics is obtained in the range of intermediate values of $g \simeq \epsilon$ (figures 1(b) and (e)). For particular values of ϵ one can see a proliferating set of periodically distributed flat regions in the dependence of the total polarization on time. In these flat regions $\langle\hat{\sigma}_z\rangle$ displays almost vanishing fluctuations around zero. The time duration of the flat regions $\delta t_{\rm TM}$ varies from $\simeq 10T$ up to $\simeq 30T$ (figures 2(a) and (b)). We coin these long-lived metastable states of the Floquet dynamics of two interacting qubits as TM states.

A detailed study of the TM dynamics results in an interesting observation: for a fixed value of g these flat regions are grouping around particular times which are periodically distributed. For example, for $g = 0.05$ and the time interval of $0 < n < 150$ we obtain two groups of flat regions of $\langle\hat{\sigma}_z\rangle$ concentrating on times around $n = 30$ and $n = 100$ (figure 2(a)). We label the flat regions with indices (k, l) as shown in figure 2(a) for $k = 1$ and 2. The dynamics of the TMs of different groups is presented in figure 2(b). We obtain that extremely small fluctuations $\Delta\langle\hat{\sigma}_z\rangle$ increase as the indices k and l grow. In particular, the fluctuations of the total polarization vary from $\Delta\langle\hat{\sigma}_z\rangle_{(1,1)}/4 \approx 0.1\%$ and $\Delta\langle\hat{\sigma}_z\rangle_{(2,2)}/4 \approx 0.25\%$ up to $\Delta\langle\hat{\sigma}_z\rangle_{(1,3)}/4 \approx 0.6\%$ and $\Delta\langle\hat{\sigma}_z\rangle_{(2,8)}/4 \approx 0.7\%$.

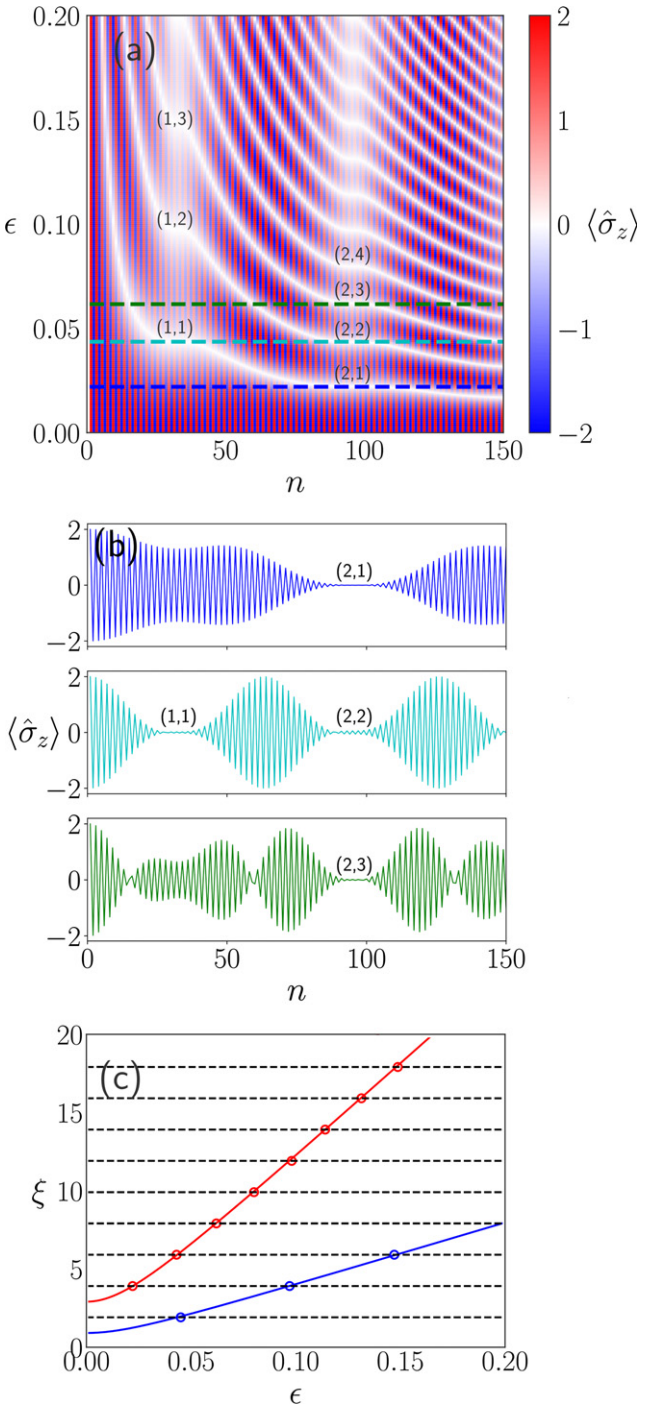

Figure 2. (a) Instantaneous total polarization $\langle\hat{\sigma}_z\rangle$ as a function of the discrete time n and the pulse imperfection ϵ for two interacting qubits with $g = 0.05$. The indices (k, l) indicate different TM states. (b) Cross-sections at the values of ϵ shown in (a) with dashed lines. (c) Generalized ratio of the quasienergies, $\xi_k = (k+1)(\pi - \epsilon_{\rm FL})/g$, as a function of ϵ for different values of commensurability parameter $k = 1$ (blue curves) and $k = 2$ (red curves). The TMs of the first (second) group are observed when ξ_k with $k = 1$ ($k = 2$) becomes an even integer (circles at the crossing points with dashed lines).

We also study the process of TM destruction as the parameter ϵ deviates from the specific values $\epsilon(k, l)$ at which the flat regions were obtained. The results for the TM $(2, 1)$ are presented in figure 3. The fluctuations of total polarization $\Delta\langle\hat{\sigma}_z\rangle$ increases linearly (blue lines in figure 3) as ϵ differs from $\epsilon(k, l)$ (the TM state obtained for $\epsilon(2, 1)$ is shown in figure 3 by the red line).

3.2. Entanglement entropy

Here, we follow the time dependence of entanglement entropy $S(nT)$ for different values of ϵ and g. Typical results are presented in the color plot of figure 4(a) for the interaction strength $g = 0.05$. The entanglement entropy demonstrates a periodic dependence on time. Since the initial state in our simulations was chosen

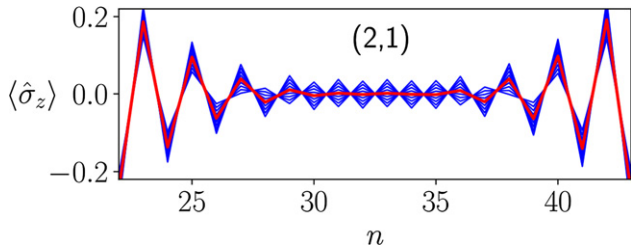

Figure 3. Instantaneous total polarization $\langle\hat{\sigma}_z\rangle$ as a function of the discrete time n for the TM $(2,1)$. The red line represents the TM for specific value $\epsilon(2,1)$ at which the flat region occurs, while the blue lines show the TM destruction as ϵ deviates from $\epsilon(2,1)$ with the maximum deviation of $\pm 1.6\%$. At the maximum deviation of ϵ we obtain the fluctuations $\Delta\langle\hat{\sigma}_z\rangle/4$ is $\simeq 0.75\%$.

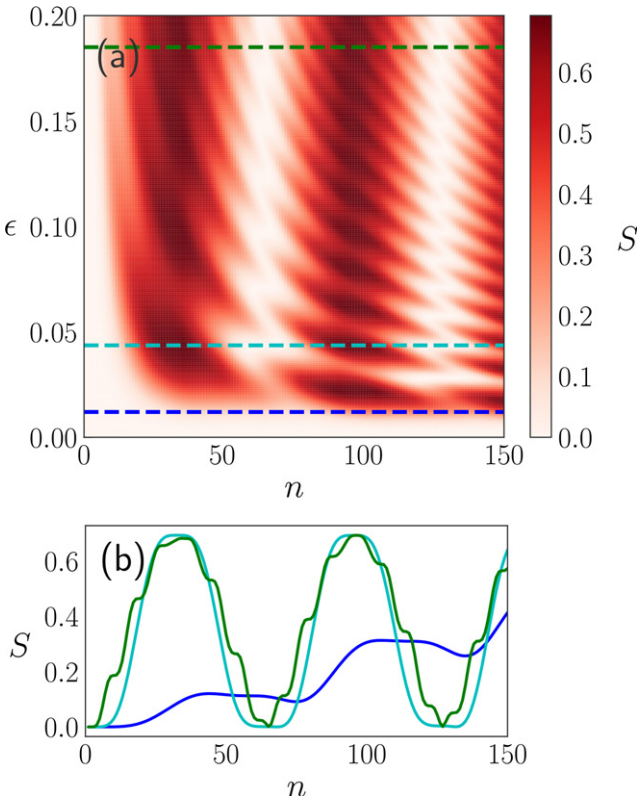

Figure 4. (a) Entanglement entropy S as a function of the discrete time n and the pulse imperfection ϵ for two interacting qubits ($g = 0.05$). (b) Cross-section of the plot in (a) at $\epsilon = 0.012$ (blue), $\epsilon = 0.0436$ (cyan), and $\epsilon = 0.185$ (green), respectively. The maximum entropy $S \simeq \ln 2$ is obtained at times where TMs are formed (figure 2).

to be a product state, we observe that at discrete times $n < 1/\epsilon$, the entanglement entropy takes small values (the left-most white regions). However, one can see that in the flat regions of $\langle\hat{\sigma}_z\rangle$, where the TMs are formed, the entanglement entropy reaches its maximum value of $S \simeq \ln 2$.

We observe various types of the time-dependence of $S(nT)$ (see figure 4(b)) which depend on the ratio of the interaction strength g and the pulse imperfection ϵ. For $g \gg \epsilon$ a slight increase of S up to some moderate value of $S \simeq 0.3$ is observed in the time region $0 < n < 150$ (blue line). For $g \ll \epsilon$, $S(nT)$ shows an additional and frequent step-like incremental and decremental modulation (green curve). The positions of the steps correspond to the stroboscopic times where the total polarization vanishes (see figure 2(a)). For $g \simeq \epsilon$ regime, $S(nT)$ performs strongly anharmonic and sharp modulations between values 0 to $\simeq \ln 2$ (or vice versa) at the stroboscopic times where the TMs start to form (or disappear). These observations indicate that the metastable TMs are in a maximally entangled state, and the value of $S \simeq \ln 2$ does not vary during the TM duration time δt_{TM}.

To explain the flat regions in the time dependence of $\langle\hat{\sigma}_z\rangle$ and the enhancement of the entanglement entropy $S(nT)$, we calculate the quasienergies and Floquet eigenstates of the periodically driven system (see appendix C and [2]). In the general case of two interacting periodically driven qubits, there are four quasienergies varying with ϵ and g. However, for this particular Floquet problem the quasienergies are fixed

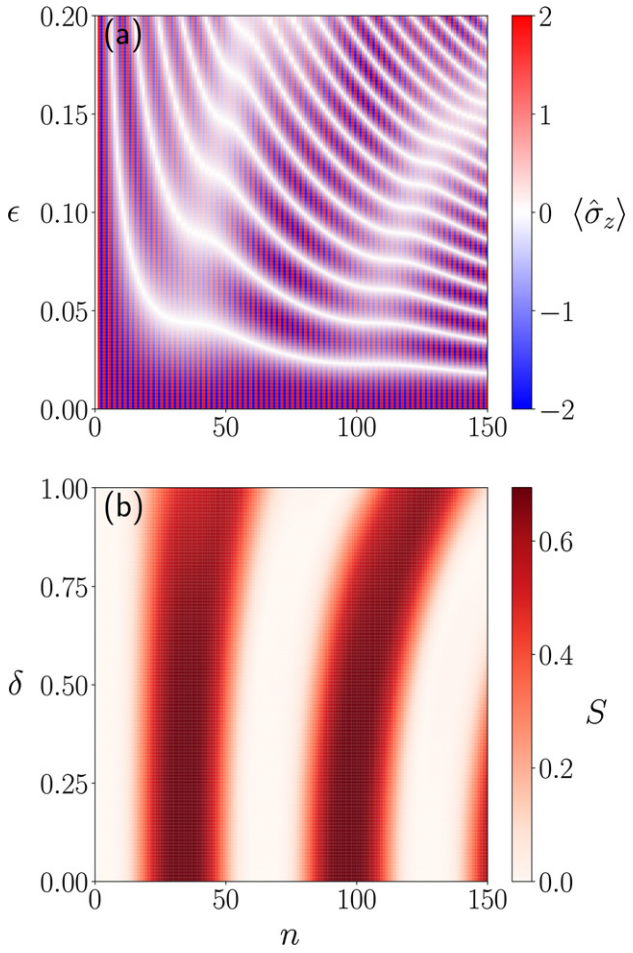

Figure 5. (a) Instantaneous total polarization $\langle\hat{\sigma}_z\rangle$ as a function of the discrete time n and the pulse imperfection ϵ for two interacting qubits in the presence of a large detuning, $\delta_1 = 0$ and $\delta_2 = 0.7$. The qubit interaction strength is set to $g = 0.05$ (b) instantaneous entanglement entropy $S(nT)$ as a function of the discrete time and the detuning δ_2 ($\delta_1 = 0$). The pulse imperfection is chosen as $\epsilon = 0.05$. The qubit interaction strength is set to $g = 0.05$.

at $E_1 = 0$; $E_2 = 2\hbar g/T$; $E_3 = \hbar\epsilon_{\rm FL}/T$; $E_4 = -\hbar(\epsilon_{\rm FL} + 2g)/T$, where a dimensionless parameter $\epsilon_{\rm FL} = \pi - g - \sqrt{g^2 + 4\epsilon^2}$ as $\{\epsilon, g\} \ll 1$ (see details in the appendix C). The Floquet dynamics shows oscillations with a few small frequencies, i.e. $\omega_1 = \pi/T - E_3/\hbar = (\pi - \epsilon_{\rm FL})/T$ and $\omega_2 = E_2/\hbar = 2g/T$, and we observe that the TMs form as the generalized ratio of these frequencies $\xi_k(\epsilon, g) = 2(k+1)\omega_1/\omega_2 = (k+1)(\pi - \epsilon_{\rm FL})/g$ is equal to ℓ, where k is the commensurability parameter, and ℓ is an even integer number. In figure 2(c) the dependencies of $\xi_k(\epsilon, g)$ for two groups of TMs with $k = 1$ and $k = 2$ are presented.

The largest entanglement entropy of the TMs is explained by inspecting the properties of the Floquet eigenstates. We find two Floquet eigenstates with maximal entanglement entropy $S = \ln 2$: $\psi_1 = (1/\sqrt{2})(|\uparrow,\uparrow\rangle - |\downarrow,\downarrow\rangle)$ and $\psi_2 = (1/\sqrt{2})(|\uparrow,\downarrow\rangle - |\downarrow,\uparrow\rangle)$. These two Floquet eigenstates form a pair of Bell states. The two remaining Floquet eigenstates $\psi_{3,4}$ have low values of S which in addition strongly depend on ϵ and g. The eigenstates ψ_1 and $\psi_{3,4}$ are symmetric with respect to a permutation of the qubits, while ψ_2 is anti-symmetric. Since the initial state is symmetric and the Hamiltonian in equation (C1) for identical qubits conserves the state symmetry, the eigenstate ψ_2 is not excited during the observed dynamics. Another important property of the Floquet eigenvectors is that the total polarization is zero in all the Floquet eigenstates. Moreover, the Floquet eigenstate ψ_1 does not vary with time (E_1 is zero). Thus, we arrive at the following scenario of the two-qubit dynamics: for finite ϵ and g the system is oscillating with period T between different states and slowly approaches the states in which $\langle\hat{\sigma}_z\rangle = 0$ (white lines in figures 1 and 2). After that, the system arrives at the TM state where the dynamics is a stroboscopic switching between the two maximally entangled Bell states: $(1/\sqrt{2})(|\uparrow,\uparrow\rangle - {\rm i}|\downarrow,\downarrow\rangle)$ and $(1/\sqrt{2})(|\uparrow,\uparrow\rangle + {\rm i}|\downarrow,\downarrow\rangle)$, and a rather slow leakage into other eigenstates. These maximally entangled Bell states are formed from the particular superposition of eigenstates ψ_1, $\psi_3 \exp[-{\rm i}E_3 nT/\hbar]$ and $\psi_4 \exp[-{\rm i}E_4 nT/\hbar]$.

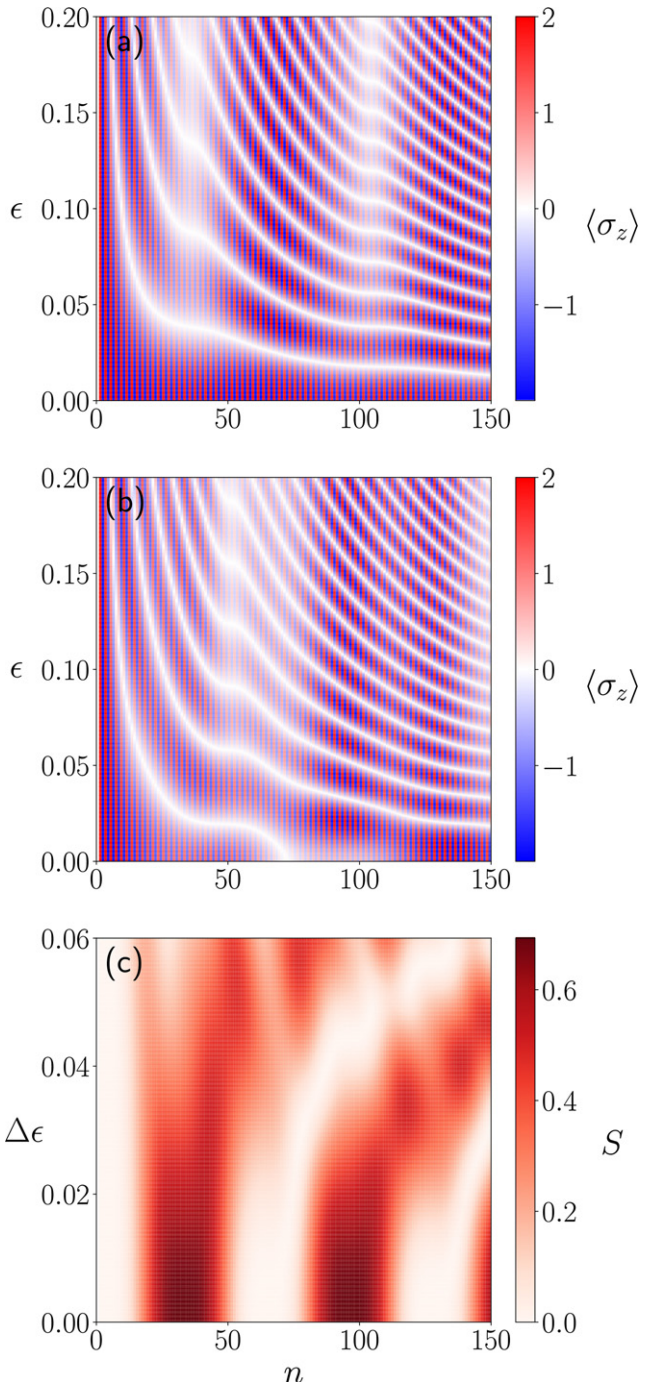

Figure 6. Instantaneous total polarization $\langle\hat{\sigma}_z\rangle$ as a function of the discrete time n and the pulse imperfection ϵ for two interacting qubits in the presence of nonuniform pulse imperfections, (a) $\Delta\epsilon = 0.02$ and (b) $\Delta\epsilon = 0.05$ (dashed lines in figure 6(c)). (c) Instantaneous entanglement entropy, $S(nT)$, as a function of the discrete time n and nonuniform pulse imperfection, $\Delta\epsilon$. The pulse imperfection was chosen as $\epsilon = 0.04$ (dashed line in figures 6(a) and (b)). The disorder in qubits frequencies is absent, and the interaction strength is set to $g = 0.05$.

3.3. Two types of disorder

So far, our numerical study was carried out for identical qubits $\delta_1 = \delta_2 = 0$. For the case of *different qubit frequencies* with $\delta_1 = 0$ and $\delta_2 = 0.7$, the dynamics of the total polarization is presented in figure 5(a). The TMs of both groups are still present, but the stroboscopic formation times of the TMs shift to larger values. Such shifts are especially pronounced for large values of ϵ (cf figures 2(a) and 5 (a)). With this type of disorder, the entanglement entropy reaches the maximum value as the TMs form. However, one can see that for the large disorder, $\delta = (\delta_2 - \delta_1) \geqslant 0.7$, the maximum value of S is slightly less than $\ln 2$ (see figure 5(b)).

We also study the Floquet dynamics of two interacting qubits in the presence of other type of disorder, namely, two slightly *different spin-flip pulses* with not equal values of ϵ_1 and ϵ_2. We observe that the Floquet

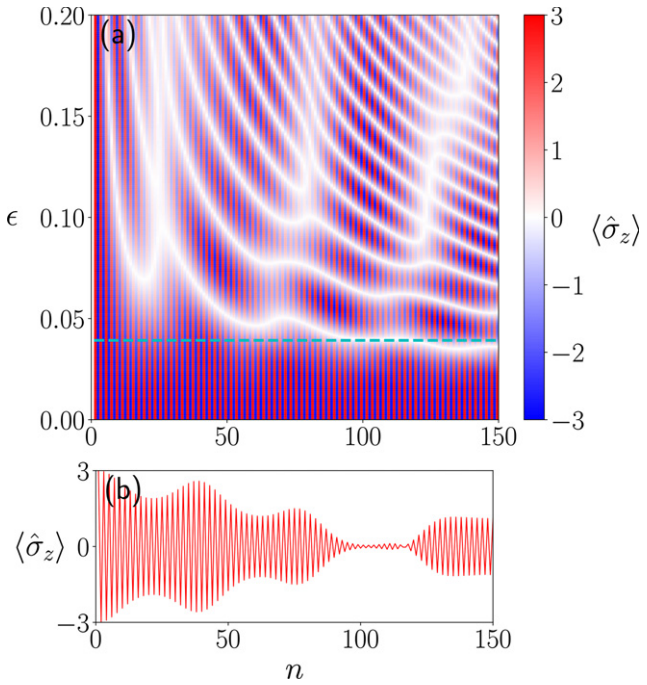

Figure 7. (a) Instantaneous total polarization $\langle\hat{\sigma}_z\rangle$ as a function of the discrete time n and the pulse imperfection ϵ for three interacting qubits. (b) Cross-section of the plot in (a) at $\epsilon = 0.04$ indicated with the dashed line in (a). The disorder in qubits frequencies is absent, and the interaction strength is set to $g = 0.05$.

Table 1. The stroboscopic evolution of the wave function $\Psi(nT)$ for four consecutive times, where the TM occurs. The parameters $g = 0.05$ and $\epsilon = 0.04$ were chosen. It corresponds to the case presented in figure 7(b). The maximally entangled GHZ states are indicated.

	Basis vectors							
Period n	$\lvert\uparrow\uparrow\uparrow\rangle$	$\lvert\downarrow\uparrow\uparrow\rangle$	$\lvert\uparrow\downarrow\uparrow\rangle$	$\lvert\downarrow\downarrow\uparrow\rangle$	$\lvert\uparrow\uparrow\downarrow\rangle$	$\lvert\downarrow\uparrow\downarrow\rangle$	$\lvert\uparrow\downarrow\downarrow\rangle$	$\lvert\downarrow\downarrow\downarrow\rangle$
100	−0.496 + 0.499i	0.005 + 0.072i	0.005 + 0.072i	−0.046 + 0.055i	0.005 + 0.072i	−0.046 + 0.055i	−0.046 + 0.055i	−0.477 − 0.497i
101	0.5 − 0.484i	−0.045 − 0.019i	−0.045 − 0.019i	−0.047 − 0.005i	−0.045 − 0.019i	−0.047 − 0.005i	−0.047 − 0.005i	−0.499 − 0.502i
102	0.507 − 0.499i	0.018 − 0.028i	0.018 − 0.028i	−0.007 − 0.028i	0.018 − 0.028i	−0.007 − 0.028i	−0.007 − 0.028i	0.488 + 0.5i
103	−0.498 + 0.49i	0.005 − 0.03i	0.005 − 0.03i	0.012 + 0.033i	0.005 − 0.03i	0.012 + 0.033i	0.012 + 0.033i	0.496 + 0.509i

dynamic does not change for $\Delta\epsilon = |\epsilon_2 - \epsilon_1| \leqslant g$ (figure 6(a)) and shows a great distortion in the opposite limit of $\Delta\epsilon \geqslant g$ (figure 6(b)). The maximum of entanglement entropy, $S(nT)$, is diminished with $\Delta\epsilon$ (see, figure 6(c)).

3.4. Floquet dynamics of chains of interacting qubits: $N = 3$ and $N = 5$

We also carried out numerical calculations of the Floquet dynamics of interacting qubits chains with a larger number of qubits, i.e. for $N = 3$ and $N = 5$. For $N = 3$ chain of qubits the results for the instantaneous total polarization $\langle\hat{\sigma}_z\rangle$ are presented in figure 7. In figure 7(a) one can observe numerous although distorted and shifted flat regions of $\langle\hat{\sigma}_z\rangle(nT)$ indicating the presence of various TMs in chains with three interacting qubits. The typical stroboscopic time dependence of $\langle\hat{\sigma}_z\rangle(nT)$ showing the formation of TM is shown in figure 7(b).

To understand the entanglement properties of the TMs forming in the chain of three interacting qubits, we numerically calculated the stroboscopic evolution of the wave function $\Psi(nT)$ corresponding to the case presented in figure 7(b). The results for four consecutive times, $n = 100$–103, where the TM occurs, are presented in table 1. Similarly to the case of two interacting qubits the TM state demonstrates periodic switching between four highly entangled GHZ states and a slow leakage in low entangled states.

We also numerically calculate the evolution of total polarization $\langle\hat{\sigma}_z\rangle$ for chains with $N = 5$ interacting qubits figure 8. Here, there are also flat regions of total polarization $\langle\hat{\sigma}_z\rangle = 0$ in which jumps occur between states close to the GHZ state, e.g. in the region with $\epsilon = 0.088$ and $n = 105$. Notice here that for short time

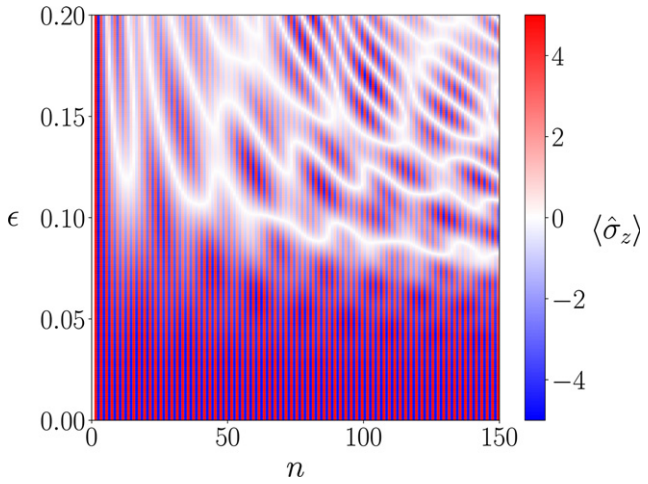

Figure 8. Instantaneous total polarization $\langle\hat{\sigma}_z\rangle$ as a function of the discrete time n and the pulse imperfection ϵ for five interacting qubits. The disorder in qubits frequencies is absent, and the interaction strength is set to $g = 0.05$.

dynamics the range of parameters ϵ, where stable oscillations with the period $2T$ are observed, is greatly extended with an increased number of qubits (compare figures 2(a), 7 (a) and 8). These oscillations indicate the appearance of the time-ordering in a system with a few interacting qubits. For larger values of ϵ the flat regions are shifted and distorted forming complex patterns in time-space domain.

3.5. Experimental proposal for the TMs observation

The TM states can be directly observed in microwave experiments with an array of interacting superconducting transmon qubits. In such a setup the periodic sequence of ac pulses is applied to each qubit. The frequency of ac pulses ω has to be chosen close to the qubit frequencies ω_i and the amplitude of the pulses determines the amplitude α in equation (C1). The spread of parameters reads $\delta_i = \omega - \omega_i$. The qubit population imbalance (total polarization) $\langle\hat{\sigma}_z\rangle$ can be directly measured with a dispersive readout regularly used for the study of quantum dynamics of superconducting qubit networks [32–34].

4. Conclusions

In conclusion, we provided numerical evidence and studied in detail a novel coherent quantum-mechanical interference phenomenon where two interacting qubits subject to a periodic sequence of $\pi - 2\epsilon$ pulses with the period T, form the time-molecule states. The TMs appear periodically in time and have a large duration, $\delta t_{\rm TM} \gg T$. The TM states are characterized by almost zero value of the total polarization and a strong enhancement of the entanglement entropy S up to the maximum value $S \simeq \ln 2$ indicating the presence of corresponding Bell state. We obtain that the TMs display a stroboscopic switching between the two maximally entangled Bell states and a slow leakage into other low entangled states. The TMs remain stable with detuned system parameters. Similarly to the case of two interacting qubits, the TMs were obtained in the Floquet dynamics of three interacting qubits, and these TMs demonstrate stroboscopic switching between four maximally entangled GHZ states. The forming of TMs was explained by the commensurability of the Floquet eigenvalues and the presence of maximally entangled Floquet eigenstates. The TMs can be observed in microwave experiments with an array of superconducting qubits.

Acknowledgments

This work was partly supported by the Institute for Basic Science, Project Code (IBS-R024-D1), and JST ERATO (No. JPMJER1601). MVF thanks the partial financial support of the Russian Science Foundation, Project (19-42-04137). We are grateful to Franco Nori for the name of 'time molecule' and thank Alexander Cherny for valuable discussions.

Data availability statement

The data that support the findings of this study are available upon reasonable request from the authors.

Appendix A. Evaluation of the instantaneous gate approximation for experiments

In the main text, we use an instantaneous gate approximation in which the Hamiltonian H_1 acts during the time, $t_1 \ll T$. This model means that the interaction between qubits is absent (turned off) during the time t_1. Since this approximation is rather difficult to satisfy in experiments we study the influence of this approximation on the Floquet dynamics of the TM. A simple evaluation of additional inhomogeneity that the system will receive due to the presence of additional interaction during the spin-flip pulse is $\pi * gt_1/T$. This imperfection can be viewed as an additional form of disorder that our system can withstand.

To check that, we introduce the time t_1 explicitly in the computational model, and for the ratio $T/t_1 \geqslant 10$ we still observe a stable dynamics of the TMs. Under this condition, the influence of the presence of the interaction g during the t_1 time is negligible. Therefore, the TMs can be observed in experiments e.g. with superconducting qubits using current experimental methods.

Appendix B. Entanglement entropy of two interacting qubits

The time dependence of the entanglement entropy $S(t)$ for the coherent Floquet dynamics of two interacting qubits is calculated by the following method [31, 35]. At stroboscopic times nT the wave function $\Psi(nT)$ is expressed as

$$\Psi(nT) = \sum_{i=1}^{4} C_i(nT)\psi_i, \tag{B1}$$

where the basis wave functions are $\psi_1 = |\uparrow\uparrow\rangle$, $\psi_2 = |\uparrow\downarrow\rangle$, $\psi_3 = |\downarrow\uparrow\rangle$ and $\psi_4 = |\downarrow\downarrow\rangle$. The full density matrix ρ with the dimension of 4 is constructed as following:

$$(\rho(nT))_{ij} = C_i^*(nT)C_j(nT). \tag{B2}$$

Next, we perform a partial trace operation, obtaining the 2×2 reduced density matrix $\tilde{\rho}(nT)$ written explicitly as

$$\tilde{\rho}(nT) = \begin{pmatrix} \tilde{\rho}_{11} = \rho_{1,1} + \rho_{2,2}; & \tilde{\rho}_{12} = \rho_{1,3} + \rho_{2,4} \\ \tilde{\rho}_{21} = \rho_{3,1} + \rho_{4,2}; & \tilde{\rho}_{22} = \rho_{3,3} + \rho_{4,4} \end{pmatrix}. \tag{B3}$$

Calculating the eigenvalues $\alpha_{1,2}(nT)$ of the reduced density matrix $\tilde{\rho}(nT)$ we obtain the entanglement entropy

$$S(nT) = -\sum_{i=1}^{2} |\alpha_i| \log(|\alpha_i|). \tag{B4}$$

Note that $S(nT) = 0$ in the absence of quantum entanglement [i.e. the wave function $\Psi(nT)$ becomes a separable product state]. At variance, for completely entangled states (Bell states) the entanglement entropy reaches its maximum value $S(nT) = \ln 2$.

Appendix C. The quasienergies and the Floquet eigenstates of two-interacting qubits

Here, we calculate the quasienergies of two identical interacting qubits subject to the time-periodic pulse sequence. The coherent quantum dynamics of such system is controlled by the time-periodic Hamiltonian:

$$\begin{aligned} \hat{H}_{\text{sys}} &= \hat{H}_1 + \hat{H}_2, \\ \hat{H}_1 &= \frac{\hbar\alpha}{2t_1}(\hat{\sigma}_{x,1} + \hat{\sigma}_{x,2}), \quad 0 < t < t_1, \\ \hat{H}_2 &= \frac{\hbar g}{T - t_1}(\hat{\sigma}_{x,1}\hat{\sigma}_{x,2} + \hat{\sigma}_{y,1}\hat{\sigma}_{y,2}), \quad t_1 < t < T. \end{aligned} \tag{C1}$$

The pulse parameter α is chosen to be close to the π pulse: $\alpha = \pi - 2\epsilon$, and $t_1 \ll T$. In this particular case the dynamics is determined by the discrete time unitary map as follows:

$$\hat{\Psi}(T) = \hat{F}\hat{\Psi}(0) = \left[\hat{U}_g \cdot \hat{U}_\epsilon\right] \hat{\Psi}(0), \tag{C2}$$

where the unitary operator of U_ϵ is written explicitly as

$$\hat{U}_\epsilon = \begin{pmatrix} \sin\,\epsilon & -\mathrm{i}\cos\,\epsilon \\ -\mathrm{i}\cos\,\epsilon & \sin\,\epsilon \end{pmatrix} \otimes \begin{pmatrix} \sin\,\epsilon & -\mathrm{i}\cos\,\epsilon \\ -\mathrm{i}\cos\,\epsilon & \sin\,\epsilon \end{pmatrix} \tag{C3}$$

and the unitary interaction operator of U_g is written as

$$\hat{U}_g = \begin{pmatrix} 1 & 0 & 0 & 0 \\ 0 & \cos(2g) & \mathrm{i}\sin(2g) & 0 \\ 0 & \mathrm{i}\sin(2g) & \cos(2g) & 0 \\ 0 & 0 & 0 & 1 \end{pmatrix}. \tag{C4}$$

The unitary map $\hat{F}$ has eigenvalues of the form, $\exp(-\mathrm{i}E_iT/\hbar)$, where E_i are quasienergies, and $i = 1, \ldots, 4$.

Next, we explicitly calculate the quasienergies E_i in the particular limit as $\{\epsilon, g\} \ll 1$. In this limit the matrix $\hat{F}$ is written as:

$$\hat{F} = \begin{pmatrix} 0 & -\mathrm{i}\epsilon & -\mathrm{i}\epsilon & -1 \\ -\mathrm{i}\epsilon & -2\mathrm{i}g & -1 & -\mathrm{i}\epsilon \\ -\mathrm{i}\epsilon & -1 & -2\mathrm{i}g & -\mathrm{i}\epsilon \\ -1 & -\mathrm{i}\epsilon & -\mathrm{i}\epsilon & 0 \end{pmatrix}. \tag{C5}$$

Diagonalizing the matrix $\hat{F}$ we obtain the quasienergies E_i as: $E_1 = 0$; $E_2 = 2\hbar g/T$; $E_3 = \hbar\epsilon_{\mathrm{FL}}/T$; $E_4 = -\hbar(\epsilon_{\mathrm{FL}} + 2g)/T$, where $\epsilon_{\mathrm{FL}} = \pi - g - \sqrt{g^2 + 4\epsilon^2}$. Thus, one can obtain the quasienergy $\epsilon_{\mathrm{FL}} = \pi - 2\epsilon$ for $g \ll \epsilon$ and $\epsilon_{\mathrm{FL}} = \pi - 2g - 2\epsilon^2/g$ for the opposite regime $g \gg \epsilon$.

The corresponding Floquet eigenvectors are written in an explicit form as:

$$\begin{aligned} \psi_1 &= (1/\sqrt{2})(|\uparrow,\uparrow\rangle - |\downarrow,\downarrow\rangle), \\ \psi_2 &= (1/\sqrt{2})(|\uparrow,\downarrow\rangle - |\downarrow,\uparrow\rangle), \\ \psi_3 &= (\beta/\sqrt{2(1+\beta^2)})[|\uparrow,\uparrow\rangle + |\downarrow,\downarrow\rangle - (1/\beta)(|\uparrow,\downarrow\rangle + |\downarrow,\uparrow\rangle)] \\ \psi_4 &= (1/\sqrt{2(1+\beta^2)})[|\uparrow,\uparrow\rangle + |\downarrow,\downarrow\rangle + \beta(|\uparrow,\downarrow\rangle + |\downarrow,\uparrow\rangle)], \end{aligned} \tag{C6}$$

where $\beta = (g + \sqrt{g^2 + 4\epsilon^2})/(2\epsilon)$.

The Floquet dynamics displays quantum beats with various characteristic frequencies, e.g. in the limit of $g = 0$ the quantum beats with the frequency $2(\pi - \epsilon_{\mathrm{FL}})/T$ are obtained, and as $g \gg \epsilon$ the quantum beats with an extremely small frequency $2(\pi - \epsilon_{\mathrm{FL}} - 2g)/T$ are obtained.

ORCID iDs

K V Shulga https://orcid.org/0000-0003-1422-4681

References

[1] Dittrich T, Hänggi P, Ingold G-L, Kramer B, Schön G and Zwerger W 1998 *Quantum Transport and Dissipation* vol 3 (New York: Wiley)
[2] Grifoni M and Hänggi P 1998 *Phys. Rep.* **304** 229
[3] Kohler S, Lehmann J and Hänggi P 2005 *Phys. Rep.* **406** 379
[4] Rabi I I, Zacharias J R, Millman S and Kusch P 1938 *Phys. Rev.* **53** 318
[5] Ramsey N F 1950 *Phys. Rev.* **78** 695
[6] Hahn E L 1950 *Phys. Rev.* **80** 580
[7] Nakamura Y, Pashkin Y A and Tsai J-S 2001 *Phys. Rev. Lett.* **87** 246601
[8] Vion D, Aassime A, Cottet A, Joyez P, Pothier H, Urbina C, Esteve D and Devoret M H 2003 *Fortschr. Phys.* **51** 462
[9] Bertaina S, Dutoit C-E, van Tol J, Dressel M, Barbara B and Stepanov A 2014 *Phys. Rev.* B **90** 060404
[10] Khemani V, Lazarides A, Moessner R and Sondhi S L 2016 *Phys. Rev. Lett.* **116** 250401
[11] Moessner R and Sondhi S L 2017 *Nat. Phys.* **13** 424
[12] D'Alessio L and Polkovnikov A 2013 *Ann. Phys., NY* **333** 19
[13] Lazarides A, Das A and Moessner R 2015 *Phys. Rev. Lett.* **115** 030402
[14] Ponte P, Papić Z, Huveneers F and Abanin D A 2015 *Phys. Rev. Lett.* **114** 140401
[15] Giergiel K, Miroszewski A and Sacha K 2018 *Phys. Rev. Lett.* **120** 140401
[16] Molignini P, van Nieuwenburg E and Chitra R 2017 *Phys. Rev.* B **96** 125144
[17] Osterloh A, Amico L, Falci G and Fazio R 2002 *Nature* **416** 608
[18] Amico L, Fazio R, Osterloh A and Vedral V 2008 *Rev. Mod. Phys.* **80** 517
[19] Wilczek F 2012 *Phys. Rev. Lett.* **109** 160401
[20] Watanabe H and Oshikawa M 2015 *Phys. Rev. Lett.* **114** 251603
[21] Yao N Y, Potter A C, Potirniche I-D and Vishwanath A 2017 *Phys. Rev. Lett.* **118** 030401
[22] Dykman M I 2019 *Phys. Rev.* A **100** 042101
[23] Guo L and Liang P 2020 *New J. Phys.* **22** 075003
[24] Pal S, Nishad N, Mahesh T S and Sreejith G J 2018 *Phys. Rev. Lett.* **120** 180602
[25] Khemani V, Moessner R and Sondhi S 2019 arXiv:1910.10745
[26] Ippoliti M, Kechedzhi K, Moessner R, Sondhi S L and Khemani V 2021 arXiv:2007.11602
[27] Choi S *et al* 2017 *Nature* **543** 221

[28] Zhang J et al 2017 Nature 543 217
[29] Greenberger D M, Horne M A and Zeilinger A 1989 Bell's Theorem, Quantum Theory and Conceptions of the Universe (Berlin: Springer) pp 69–72
[30] Greenberger D M, Horne M A, Shimony A and Zeilinger A 1990 Am. J. Phys. 58 1131
[31] Eisert J, Cramer M and Plenio M B 2010 Rev. Mod. Phys. 82 277
[32] Blais A, Gambetta J, Wallraff A, Schuster D I, Girvin S M, Devoret M H and Schoelkopf R J 2007 Phys. Rev. A 75 032329
[33] Majer J et al 2007 Nature 449 443
[34] Jerger M, Poletto S, Macha P, Hübner U, Il'ichev E and Ustinov A V 2012 Appl. Phys. Lett. 101 042604
[35] Dirac P A M 1930 Mathematical Proceedings of the Cambridge Philosophical Society vol 26 (Cambridge: Cambridge University Press) pp 376–85